


Enhanced magnon-magnon entanglement in the vicinity of an angular momentum compensation point of a ferrimagnet in a cavity

Jaechul Shim^{1,2} and Kyung-Jin Lee^{1,*}

¹*Department of Physics, Korea Advanced Institute of Science and Technology (KAIST), Daejeon 34141, Korea*

²*Semiconductor R&D Center, Samsung Electronics Co. Ltd., Hwaseong, Gyeonggi 18448, Korea*

 (Received 28 February 2022; revised 19 August 2022; accepted 20 October 2022; published 31 October 2022)

Highly entangled states are the key to the realization of quantum information processing. We theoretically investigate magnon-magnon entanglement in a compensated ferrimagnet. We show that the steady-state magnon-magnon entanglement largely enhances in the vicinity of angular momentum compensation point (T_A) when magnons are coupled with photons in a cavity. The origin of this enhancement is that the ground state of ferrimagnet can be close to the Einstein-Podolsky-Rosen state near T_A . This feature is unique to ferrimagnets with different Landé g factors between sublattices and makes the magnon entanglement of ferrimagnets higher than that of ferromagnets and antiferromagnets. Our result will invigorate research on quantum information processing based on magnon-magnon entanglement.

DOI: [10.1103/PhysRevB.106.L140408](https://doi.org/10.1103/PhysRevB.106.L140408)

Introduction. Quantum information processing (QIP) [1,2] describes the manipulation of quantum information, utilizing the quantum nature of system. Representative subdisciplines of QIP include (quantum-) computing, cryptography, teleportation, and simulation [2,3], which provide innovative strategies to overcome classical limitations of each research field. As quantum entanglement is the vital resource to perform various quantum tasks [3–5], high entanglement is the key to the realization of QIP.

For continuous-variable quantum information [4–6], entanglement can be generated through squeezing [4,5] as was investigated in optics [2], optomechanics [7], and atomic ensembles [8]. Recent studies reveal that magnons also have notable entanglement through the squeezing [9–15]. Moreover, the entanglement between magnons and other quasiparticles (i.e., magnon-photon [16–18], magnon-phonon [19], and magnon-superconducting qubit [20,21]) are of current interest. These studies open a field named quantum magnonics [22–26] that utilizes magnetic systems as a platform for QIP. In particular, two-mode squeezed states of magnon in antiferromagnets (AFMs) attract attention [11,14] because squeezed magnon states inherently arise due to antiferromagnetic exchange coupling in equilibrium. Moreover, large exchange coupling of AFMs [27–29] gives rise to large squeezing effect and associated high magnon-magnon entanglement [11]. However, the squeeze parameter r , a measure of the amount of squeezing, and the associated magnon-magnon entanglement of AFMs are fundamentally limited by the magnetic anisotropy [11] that is always present in magnetic materials.

The ideal Einstein-Podolsky-Rosen (EPR) state [30] is a state that is perfectly correlated and maximally entangled, but unphysical as it has infinite energy [5]. The EPR state corresponds to infinite squeezing ($r \rightarrow \infty$), resulting in in-

finite entanglement. Although the EPR state is unachievable in reality, it is of crucial importance to find a system where the ground state approaches the EPR state as close as possible because the ground-state entanglement, which is defined in the absence of dissipation and noise, provides a guideline of the maximal steady-state entanglement allowed in the system in the presence of dissipation and noise.

In this Letter, we show that the magnon ground state of antiferromagnetically coupled ferrimagnets (FIMs) near the angular momentum compensation point T_A approaches the EPR state by the Zeeman coupling. This feature is unique to FIMs where the Landé g factors are different between two sublattices and thus is absent in AFMs where the Landé g factors are the same. At T_A , the different Landé g factors of FIM result in zero net angular momentum [i.e., $\delta_s = s_b - s_a = 0$ where $s_a(s_b)$ is the angular momentum at the sublattice $a(b)$] but finite magnetic moment, which allows for antiferromagnetic spin dynamics due to $\delta_s = 0$ with finite Zeeman coupling due to nonzero net magnetic moment [31–34]. This Zeeman coupling cancels the magnetic anisotropy effect, which is detrimental for the entanglement by limiting r , and realizes the magnon ground state close to the EPR state. As a result, with magnon-photon coupling [35–48], the steady-state magnon-magnon entanglement enhances near T_A . The enhanced entanglement near T_A is maintained regardless of bath temperature. Importantly, FIMs near T_A exhibits higher magnon entanglement than AFMs and ferromagnets (FMs).

Ground-State Magnon Entanglement Enhanced by Approaching the EPR State. We consider a collinear FIM consisting of two sublattices a and b . The Hamiltonian of FIM is [49]

$$\begin{aligned} \hat{\mathcal{H}} = & 2J \sum_{l,m} \hat{\mathbf{S}}_l \cdot \hat{\mathbf{S}}_m - \sum_l \hbar\gamma_a(\mathbf{B}_0 + \mathbf{B}_{K,a}) \cdot \hat{\mathbf{S}}_l \\ & - \sum_m \hbar\gamma_b(\mathbf{B}_0 + \mathbf{B}_{K,b}) \cdot \hat{\mathbf{S}}_m, \end{aligned} \quad (1)$$

*kjlee@kaist.ac.kr

where $J > 0$ is the exchange constant, $\hat{\mathbf{S}}_{l(m)}$ is the spin on site $l(m)$ of sublattice $a(b)$, \mathbf{B}_0 is the external magnetic field along the z axis, \mathbf{B}_K is the uniaxial anisotropy field along the z axis, and $\gamma = g_L \mu_B / \hbar$ is the gyromagnetic ratio with the Landé g factor g_L and the Bohr magneton μ_B . The subscript $a(b)$ represents the sublattice $a(b)$.

Using the Holstein-Primakoff (HP) transformation [50], we convert the spin operators $\hat{\mathbf{S}}_{l(m)}$ to the bosonic annihilation \hat{a}_l (\hat{b}_m) and creation operators \hat{a}_l^\dagger (\hat{b}_m^\dagger). For the uniform mode (i.e., wavevector = 0), the Hamiltonian is rewritten as

$$\hat{H} = A_1(\hat{a}^\dagger \hat{a} + \hat{b}^\dagger \hat{b}) + A_2(\hat{a}^\dagger \hat{a} - \hat{b}^\dagger \hat{b}) + A_3(\hat{a}^\dagger \hat{b}^\dagger + \hat{a} \hat{b}), \quad (2)$$

with

$$\begin{aligned} A_1 &= \frac{1}{2} \left[\hbar \gamma_a B_a - \hbar \gamma_b B_b + \left(\sqrt{\frac{S_a}{S_b}} + \sqrt{\frac{S_b}{S_a}} \right) J_0^{ab} \right], \\ A_2 &= \frac{1}{2} \left[\hbar \gamma_a B_a + \hbar \gamma_b B_b - \left(\sqrt{\frac{S_a}{S_b}} - \sqrt{\frac{S_b}{S_a}} \right) J_0^{ab} \right], \\ A_3 &= J_0^{ab}, \end{aligned}$$

where S_i is the magnitude of spin vector, $B_a = B_0 + 2K_u/\gamma_a s_a$ ($B_b = B_0 - 2K_u/\gamma_b s_b$) is the sum of the external field and the anisotropy field at sublattice $a(b)$, $K_u > 0$ is the anisotropy energy density, $s = \hbar S/d^3$ is the spin density, d is the lattice constant, $J_0^{ab} = 2\sqrt{S_a S_b} J z$ is the effective exchange, and z is the coordination number.

The Hamiltonian [Eq. (2)] is diagonalized via the Bogoliubov transformation [51,52] with two Bogoliubov modes $\hat{\alpha} = u\hat{a} + v\hat{b}^\dagger$ and $\hat{\beta} = u\hat{b} + v\hat{a}^\dagger$, where $\hat{\alpha}$ and $\hat{\beta}$ preserve the bosonic commutation relations. This Bogoliubov transformation can be rephrased with the two-mode squeezing operator $\hat{S}(r) = \exp(r\hat{a}\hat{b} - r\hat{a}^\dagger\hat{b}^\dagger)$ [11,52] as $\hat{S}(r)\hat{a}\hat{S}^\dagger(r) = \hat{\alpha}$, $\hat{S}(r)\hat{b}\hat{S}^\dagger(r) = \hat{\beta}$. Accordingly, u and v are defined with the squeeze parameter ($r > 0$) as $u \equiv \cosh(r/2)$, $v \equiv \sinh(r/2)$. Then, the Hamiltonian is transformed to

$$\hat{H} = \omega_\alpha \hat{\alpha}^\dagger \hat{\alpha} + \omega_\beta \hat{\beta}^\dagger \hat{\beta}, \quad (3)$$

where $\omega_\alpha = A_2 + \sqrt{A_1^2 - A_3^2}$ and $\omega_\beta = -A_2 + \sqrt{A_1^2 - A_3^2}$ are the eigenvalues of the squeezed magnon modes of FIMs. One can reproduce the eigenvalues of the squeezed magnon modes of AFM by setting $s_a = s_b$ and $\gamma_a = \gamma_b$.

The ground state of FIM is a two-mode squeezed vacuum state as in AFM [11], given as

$$|\hat{\alpha}^\dagger \hat{\alpha} = 0, \hat{\beta}^\dagger \hat{\beta} = 0\rangle_{\text{sq}} = \hat{S}(r)|0, 0\rangle, \quad (4)$$

where $|0, 0\rangle_{\text{sq}}$ is a two-mode squeezed vacuum state and $|0, 0\rangle$ is a double vacuum state. From the above Bogoliubov transformation, we find r for FIM as

$$r = \tanh^{-1} \zeta, \quad (5)$$

where

$$\begin{aligned} \zeta &= \frac{A_3}{A_1} = \frac{2J_0^{ab}}{\hbar \gamma_a B_a - \hbar \gamma_b B_b + \left(\sqrt{\frac{S_a}{S_b}} + \sqrt{\frac{S_b}{S_a}} \right) J_0^{ab}} \\ &= \frac{2J \sqrt{S_a S_b} z}{K_u V (S_a^{-1} + S_b^{-1}) + J(S_a + S_b)z - \delta_\gamma \hbar B_0 / 2}. \end{aligned} \quad (6)$$

Here $\delta_\gamma = \gamma_b - \gamma_a = (g_{L,b} - g_{L,a})\mu_B/\hbar > 0$ is the difference of the gyromagnetic ratios between two sublattices and $V = d^3$ is the unit volume. The ground-state entanglement $E_N^{(g)}$ of FIM is calculated using the logarithmic negativity [6] in the absence of dissipation and noise. For a two-mode squeezed state, $E_N^{(g)}$ is simply given as $2r$ [14]. Therefore, Eq. (6) describes how $E_N^{(g)}$ of FIM varies with material properties and external field B_0 .

The EPR state corresponds to $r = \infty$ that is equivalent to $\zeta = 1$. From Eq. (6), we obtain the EPR field B_{EPR} that makes $\zeta = 1$:

$$B_{\text{EPR}} = \frac{1}{\delta_\gamma} \left[\frac{2(s_t - \sqrt{s_t^2 - \delta_s^2})JzV}{\hbar^2} + \frac{8K_u s_t}{s_t^2 - \delta_s^2} \right], \quad (7)$$

where $s_t = s_b + s_a$ is the sum of the spin density.

Equations (6) and (7) show a critical role of δ_γ in $E_N^{(g)}$. Only with $\delta_\gamma \neq 0$ (i.e., $g_{L,a} \neq g_{L,b}$), $E_N^{(g)}$ is tunable with B_0 and, more importantly, B_{EPR} is finite. For AFMs ($\delta_\gamma = 0$ and $\delta_s = 0$), $E_N^{(g)}$ does not depend on B_0 and $B_{\text{EPR}} (\propto K_u/\delta_\gamma)$ is infinite due to the combined effect of nonzero magnetic anisotropy and zero δ_γ so that one cannot approach the EPR state. Accordingly, $E_N^{(g)}$ of AFM is relatively small. As far as the EPR state is concerned, FIMs with $\delta_\gamma = 0$ are qualitatively same as AFMs. In contrast, the Zeeman coupling takes effect for FIMs with $\delta_\gamma \neq 0$ so that B_{EPR} is finite and the EPR state can be approached by applying B_0 . We note that B_{EPR} is minimized at T_A (i.e., $\delta_s = 0$) [see Eq. (7)] because it is independent of the exchange J , which is much larger than the anisotropy K_u . As a result, EPR state can be approached with an experimentally accessible magnetic field at T_A . We note that a recent study investigated the magnon entanglement in FIMs with $\delta_\gamma = 0$ [15] so that it is irrelevant to the EPR state and the entanglement is relatively small.

In reality, the EPR state is unachievable because it is unphysical. In FIMs, the spin-flop transition [53], which is nearly 90° rotation of the sublattice moments due to B_0 , prevents one from realizing the exact EPR state. In our model, B_0 corresponding to $\omega_\beta = 0$ gives the spin-flop field B_{SF} [Supplementary Note 1 (SN-1) in the Supplemental Materials [54] (see also Refs. [55–61] therein)]. In the limit of small anisotropy compared to exchange (i.e., $\hbar^2 K_u / s_t^2 J V z \equiv \eta \ll 1$), B_{SF} is approximated as

$$B_{\text{SF}} = \frac{8K_u}{\gamma_t \delta_s + \delta_\gamma s_t} \left(1 - \eta \frac{2s_t^2 (\gamma_t s_t + \delta_\gamma \delta_s)^2}{(s_t^2 - \delta_s^2) (\gamma_t \delta_s + \delta_\gamma s_t)^2} \right), \quad (8)$$

where $\gamma_t = \gamma_a + \gamma_b$. Equation (8) shows that at T_A where B_{EPR} minimizes, the spin-flop field becomes $B_{\text{SF}} = B_{\text{EPR}} (1 - 2\eta \gamma_t^2 / \delta_\gamma^2)$. Given $\eta \ll 1$, B_{SF} approaches B_{EPR} at T_A unless $\delta_\gamma \ll \gamma_t$.

Figure 1(a) shows $E_N^{(g)}$ ($= 2r$) as a function of B_0 for an AFM and a FIM with $\delta_\gamma \neq 0$. $E_N^{(g)}$ of AFM (grey line) does not vary with B_0 because $\delta_\gamma = 0$. On the other hand, $E_N^{(g)}$ of FIM (black line) increases with B_0 and goes to the infinity at $B_0 = B_{\text{EPR}}$. Note that $E_N^{(g)}$ of FIM consists of solid and dotted lines. The only solid line is meaningful because the dotted line corresponds to the field ranges where the spin-flop transition occurs. As the linear approximation of the HP transformation

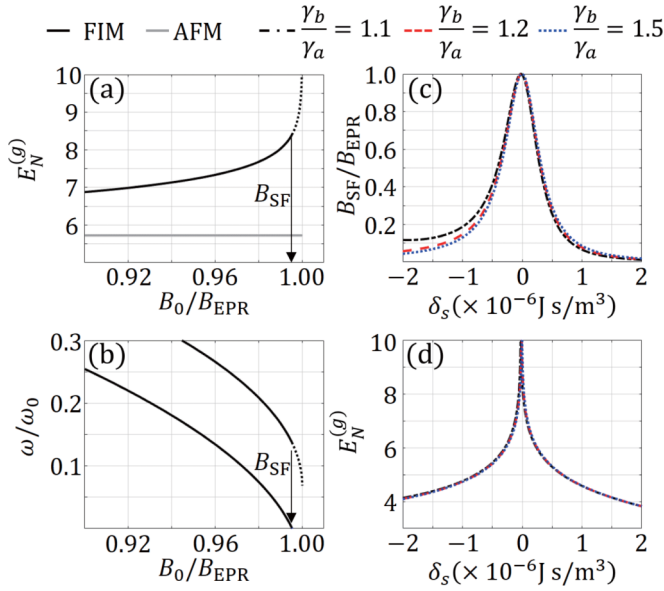


FIG. 1. (a) $E_N^{(g)}$ of an AFM (grey line, $\gamma_b/\gamma_a = 1.0$) and a FIM (black line, $\gamma_b/\gamma_a = 1.1$) as a function of B_0 . (b) Dispersions of two Bogoliubov modes (α and β ; $\omega_\alpha < \omega_\beta$) as a function of B_0/B_{EPR} for FIM. ω_0 is the frequency of α mode at $B_0 = 0$. (c) B_{SF}/B_{EPR} as a function of δ_s for different values of γ_b/γ_a . (d) Maximum $E_N^{(g)}$ as a function of δ_s for different values of γ_b/γ_a . Other parameters: $\delta_s = 0$ for (a) and (b), $s = 5.3 \times 10^{-5} \text{ J s/m}^3$, $A_{ex} (= JS_a S_b/d) = 5 \times 10^{-12} \text{ J/m}$, $z = 6$, $d = 4 \times 10^{-10} \text{ m}$, $\gamma_a = 1.76 \times 10^{11} \text{ rad/(secT)}$, and $K_a = 4 \times 10^3 \text{ J/m}^3$. Parameters for FIMs are based on Ref. [62].

is valid for $B_0 < B_{SF}$, the enhanced $E_N^{(g)}$ by approaching the EPR state is valid only for $B_0 < B_{SF}$.

As $E_N^{(g)}$ of FIM diverges at $B_0 = B_{EPR}$ and B_0 is limited by B_{SF} , the maximally enhanced $E_N^{(g)}$ is achieved for a condition that B_{SF} approaches B_{EPR} as close as possible. This condition is realized in the vicinity of T_A : As shown in Fig. 1(c), B_{SF} is close to B_{EPR} in the vicinity of T_A . As a result, $E_N^{(g)}$ maximizes in the vicinity of T_A as well [Fig. 1(d)].

Steady-State Magnon Entanglement in a Cavity. As dissipation and noise are always present, the entanglement that can be probed in an experiment is the steady-state entanglement $E_N^{(s)}$, not the ground-state entanglement $E_N^{(g)}$. In this section, we show that approaching the EPR state of FIMs with $\delta_\gamma \neq 0$ enhances $E_N^{(s)}$ of magnons when magnons are coupled with photons. To this end, we calculate $E_N^{(s)}$ of magnons without and with photon in the presence of dissipation and noise.

We introduce the dissipation term $\kappa_{a(b)}$, which quantifies the interaction between the magnon mode $\hat{a}(\hat{b})$ and the environment [14]. We assume that the dissipation rates of two modes are the same ($\kappa_a = \kappa_b = \kappa_m$). We also consider the noise from the environment, \hat{a}_n and \hat{b}_n . Adopting the fluctuation-dissipation theorem [63], the quantum Langevin equations govern how the quantum state evolves with time:

$$\begin{aligned} \frac{d\hat{a}}{dt} &= -(\kappa_m + i\omega_a)\hat{a} - iA_3\hat{b}^\dagger + \sqrt{2\kappa_m}\hat{a}_n \\ \frac{d\hat{b}}{dt} &= -(\kappa_m + i\omega_b)\hat{b} - iA_3\hat{a}^\dagger + \sqrt{2\kappa_m}\hat{b}_n, \end{aligned} \quad (9)$$

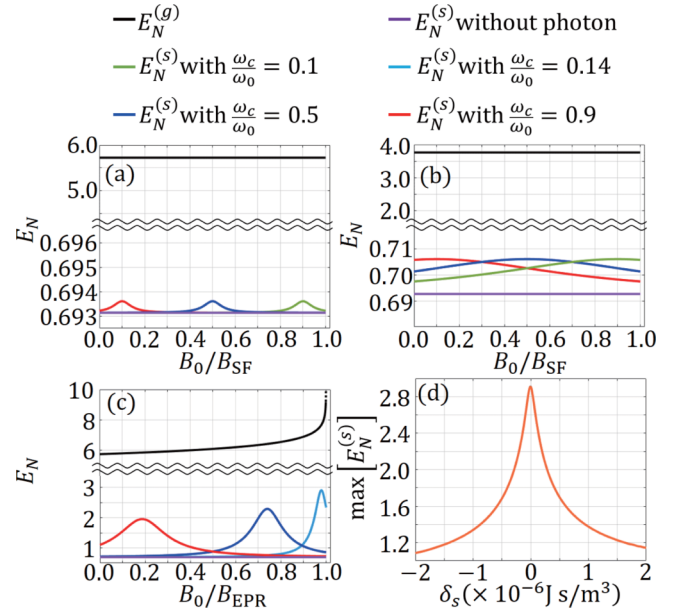


FIG. 2. $E_N^{(g)}$ and $E_N^{(s)}$ as a function of B_0 for (a) AFM, (b) FIM1 with $\gamma_b/\gamma_a = 1$, and (c) FIM2 with $\gamma_b/\gamma_a = 1.5$. (d) Maximum $E_N^{(s)}$ of FIM2 with $\gamma_b/\gamma_a = 1.5$ as a function of δ_s . For (a) and (c) $\delta_s = 0$, $s = 5.3 \times 10^{-5} \text{ J sec/m}^3$. For (b) $\delta_s = 2.1 \times 10^{-6} \text{ J sec/m}^3$, $s = 4.6 \times 10^{-5} \text{ J sec/m}^3$. For (d) $s = -3.4 \times \delta_s + 5.3 \times 10^{-5} \text{ J sec/m}^3$. Common parameters: $g_{ac} = 3 \times 10^{-5} A_3$, $\kappa_m = 0.33 g_{ac}$, and $\kappa_c = 10 g_{ac}$. Other parameters are the same with those in Fig. 1.

where $\omega_a (= A_1 + A_2)$ and $\omega_b (= A_1 - A_2)$ are eigenvalues of the modes \hat{a} and \hat{b} , respectively. Interacting with noisy environments, the ground state given in Eq. (4) eventually becomes a steady Gaussian state.

Based on the covariance matrix using the Lyapunov equation [7, 14], $E_N^{(s)}$ without photon is given as (SN-2 [54])

$$E_N^{(s)} = \max \left[0, \frac{1}{2} \ln \left(1 + \frac{A_3(A_3 + 2\sqrt{A_1^2 + \kappa_m^2})}{A_1^2 + \kappa_m^2} \right) \right]. \quad (10)$$

Figure 2 shows $E_N^{(g)}$ (black lines) and $E_N^{(s)}$ without photon (purple lines) as a function of B_0 for (a) AFM, (b) FIM1 with $\delta_\gamma = 0$, and (c) FIM2 with $\delta_\gamma \neq 0$. For all cases, $E_N^{(s)}$ without photon is close to $0.69 [\approx \ln(2)]$ regardless of B_0 . This means that the noise and dissipation reduce $E_N^{(s)}$ when there is no photon in the system. In particular, the important feature of FIM2, i.e., a rapid increase of $E_N^{(g)}$ by approaching the EPR state, disappears for $E_N^{(s)}$ without photon.

In order to recover this important feature, we consider the coupling between squeezed magnons with circularly polarized microwave photons as the magnon-photon coupling enhances the entanglement between magnons [14, 15]. Due to the angular momentum conservation, circularly polarized photons have a beam-splitter-type interaction with one magnon mode and a parametric type interaction with the other magnon mode (SN-3 [54]). Through the beam-splitter-type interaction, photons cool down one magnon mode toward its ground state [Eq. (4)], thereby recovering the feature of $E_N^{(g)}$ for that magnon mode, i.e., the enhanced magnon entanglement by ap-

proaching the EPR state. Consequently, this feature is partially recovered for $E_N^{(s)}$ with photon, as shown below.

The Hamiltonian of photon coupled magnon system where $\hat{b}(\hat{a})$ magnon mode for the beam-splitter (parametric) type interaction is written as (SN-3 [54])

$$\begin{aligned} \hat{H}_{m-p} = & \omega_a \hat{a}^\dagger \hat{a} + \omega_b \hat{b}^\dagger \hat{b} + g_{ab}(\hat{a}^\dagger \hat{b}^\dagger + \hat{a} \hat{b}) \\ & + \omega_c \hat{c}^\dagger \hat{c} + g_{ac}(\hat{a}^\dagger \hat{c}^\dagger + \hat{a} \hat{c}) + g_{bc}(\hat{b}^\dagger \hat{c} + \hat{b} \hat{c}^\dagger), \end{aligned} \quad (11)$$

of which Bogoliubov transformed form is

$$\begin{aligned} \tilde{H}_{m-p} = & \omega_a \hat{\alpha}^\dagger \hat{\alpha} + \omega_\beta \hat{\beta}^\dagger \hat{\beta} + \omega_c \hat{c}^\dagger \hat{c} \\ & + g_{\alpha c}(\hat{\alpha}^\dagger \hat{c}^\dagger + \hat{\alpha} \hat{c}) + g_{\beta c}(\hat{\beta}^\dagger \hat{c} + \hat{\beta} \hat{c}^\dagger), \end{aligned} \quad (12)$$

where $\hat{c}(\hat{c}^\dagger)$ is the annihilation (creation) operator for photons, ω_c is the photon frequency, and $g_j (j = ab, ac, bc, \alpha c, \beta c)$ is the coupling strength between two modes represented by subindices [14]. Here g_{bc}/g_{ac} is $(\gamma_b/\gamma_a)\sqrt{S_b/S_a}$ [37].

The quantum Langevin equations for the three-mode system are:

$$\begin{aligned} \frac{d\hat{a}}{dt} = & -(\kappa_m + i\omega_a)\hat{a} - iA_3\hat{b}^\dagger - ig_{ac}\hat{c}^\dagger + \sqrt{2\kappa_m}\hat{a}_n, \quad (13) \\ \frac{d\hat{b}}{dt} = & -(\kappa_m + i\omega_b)\hat{b} - iA_3\hat{a}^\dagger - ig_{bc}\hat{c} + \sqrt{2\kappa_m}\hat{b}_n, \\ \frac{d\hat{c}}{dt} = & -(\kappa_c + i\omega_c)\hat{c} - ig_{ac}\hat{a}^\dagger - ig_{bc}\hat{b} + \sqrt{2\kappa_c}\hat{c}_n, \end{aligned}$$

where κ_c is the dissipation rate of the photon mode. Numerically solving the Lyapunov equation based on Eq. (13) gives $E_N^{(s)}$ between magnon modes of the photon coupled system (SN-4 [54]). Note that we check the stability of the steady state using the Routh-Hurwitz criterion [64].

Figure 2 shows $E_N^{(s)}$ with photon at various photon frequencies (red, blue, green, and light-blue lines) as a function of B_0 for (a) AFM, (b) FIM1 with $\delta_\gamma = 0$, and (c) FIM2 with $\delta_\gamma \neq 0$. For all cases, $E_N^{(s)}$ with photon is larger than $E_N^{(s)}$ without photon because the magnon-photon coupling cools down one magnon mode. The important observation is that only for (c) FIM2 with $\delta_\gamma \neq 0$, $E_N^{(s)}$ with photon increases when B_0 approaches B_{EPR} , whereas for (a) AFM and (b) FIM1, $E_N^{(s)}$ with photon is independent of B_0 . This result confirms that the enhanced $E_N^{(g)}$ by approaching the EPR state is partially recovered in $E_N^{(s)}$ with photon for FIMs with $\delta_\gamma \neq 0$.

Although this recovery is not perfect due to dissipation and noise, the enhancement of $E_N^{(s)}$ is substantial. As shown above, B_{SF} is close to B_{EPR} near T_A [Fig. 1(c)]. Therefore, it is expected that applying $B_0 \approx B_{SF}$ results in a maximal enhancement of $E_N^{(s)}$ with photon near T_A . To check this ex-

pectation, we calculate the maximum $E_N^{(s)}$ with photon, which is obtained at $B_0 \approx B_{SF}$, as a function of δ_γ . Figure 2(d) shows that $E_N^{(s)}$ with photon maximizes in the vicinity of T_A .

Discussion. In this Letter, we theoretically show that the magnon ground state of a compensated FIM can be close to the EPR state. This feature maximizes both ground-state and steady-state magnon-magnon entanglements near T_A . Consequently, FIMs near T_A exhibit higher magnon entanglement than FMs and AFMs (SN-5 [54]). This conclusion is obtained with three assumptions: zero bath temperature, a fixed photon decay rate (κ_c), and the same dissipation rates for two magnon modes ($\kappa_a = \kappa_b$). In the Supplementary Material (SN-6 and SN-7) [54], we show that the conclusion is valid even with relaxing these assumptions, evidencing that our result is a general phenomenon.

For an experimental realization of our prediction, FIMs must satisfy two conditions (SN-8 [54]): First, net magnetic moment is finite while net angular momentum nearly vanishes. This condition is satisfied for rare earth (RE)-transition metal (TM) FIMs because of the different Landé g factors between the RE and TM elements [32,65]. RE-doped ferrimagnetic insulators (i.e., Bi-doped $Y_3Fe_5O_{12}$) also approximately satisfy this condition [66]. The second condition is that T_A must be kept around 1 K because the magnon entanglement vanishes at high temperature. This second condition can be satisfied by controlling the relative composition between the RE and TM elements. For such FIMs, the measurements of spin noise [67] or spin current noise [9] could experimentally probe our prediction (SN-9 [54]).

Our result suggests that FIMs with $\delta_\gamma \neq 0$ could serve as a material platform for generating high and tunable entanglement in hybrid quantum systems [68] for QIP. As magnons correspond to continuous-variable quantum information as photons do, any quantum applications that have been demonstrated with photons can in principle be done with magnons. Given that quantum magnonics is an emerging field, there are many unexplored theoretical and experimental tasks for quantum magnonics. However, it does not mean that quantum magnonics could only mimic quantum optics. In addition to the large squeeze parameter of FIMs that we report here, an important difference of squeezed state of magnon from squeezed state of light is its equilibrium nature, i.e., the magnon squeezing results from energy minimization [24]. The equilibrium nature of squeezed magnon may yield qualitative differences from the nonequilibrium squeezing physics of light [24], which remains unexplored and thus demands further investigation.

Acknowledgments. This work was supported by Samsung Research Funding Center of Samsung Electronics under Project No. SRFCMA1702-02.

- [1] T. P. Spiller, *Proc. IEEE* **84**, 1719 (1996)
 [2] F. Flamini, N. Spagnolo, and F. Sciarrino, *Rep. Prog. Phys.* **82**, 016001 (2019).

- [3] M. A. Nielsen and I. L. Chuang, *Quantum Computation and Quantum Information* (Cambridge University Press, Cambridge, UK, 2000).

- [4] S. L. Braunstein and A. K. Pati, *Quantum Information with Continuous Variables* (Kluwer Academic Publishers, The Netherlands, 2003).
- [5] S. L. Braunstein and P. van Loock, *Rev. Mod. Phys.* **77**, 513 (2005).
- [6] G. Adesso and F. Illuminati, *J. Phys. A: Math. Theor.* **40**, 7821 (2007).
- [7] D. Vitali, S. Gigan, A. Ferreira, H. R. Böhm, P. Tombesi, A. Guerreiro, V. Vedral, A. Zeilinger, and M. Aspelmeyer, *Phys. Rev. Lett.* **98**, 030405 (2007).
- [8] L.-M. Duan, J. I. Cirac, P. Zoller, and E. S. Polzik, *Phys. Rev. Lett.* **85**, 5643 (2000).
- [9] A. Kamra and W. Belzig, *Phys. Rev. Lett.* **116**, 146601 (2016).
- [10] A. Kamra and W. Belzig, *Phys. Rev. B* **94**, 014419 (2016).
- [11] A. Kamra, E. Thingstad, G. Rastelli, R. A. Duine, A. Brataas, W. Belzig, and A. Sudbø, *Phys. Rev. B* **100**, 174407 (2019).
- [12] Z. Zhang, M. O. Scully, and G. S. Agarwal, *Phys. Rev. Res.* **1**, 023021 (2019).
- [13] J. Zou, S. K. Kim, and Y. Tserkovnyak, *Phys. Rev. B* **101**, 014416 (2020).
- [14] H. Y. Yuan, S. Zheng, Z. Ficek, Q. Y. He, and M. H. Yung, *Phys. Rev. B* **101**, 014419 (2020).
- [15] S.-S. Zheng, F.-X. Sun, H.-Y. Yuan, Z. Ficek, Q.-H. Gong, and Q.-Y. He, *Sci. China Phys. Mech. Astron.* **64**, 210311 (2021).
- [16] H. Y. Yuan, P. Yan, S. Zheng, Q. Y. He, K. Xia, and M.-H. Yung, *Phys. Rev. Lett.* **124**, 053602 (2020).
- [17] F.-X. Sun, S.-S. Zheng, Y. Xiao, Q. Gong, Q. He, and K. Xia, *Phys. Rev. Lett.* **127**, 087203 (2021).
- [18] S. Sharma, V. A. S. V. Bittencourt, A. D. Karenowska, and S. V. Kusminskiy, *Phys. Rev. B* **103**, L100403 (2021).
- [19] X. Zhang, C.-L. Zou, L. Jiang, and H. X. Tang, *Sci. Adv.* **2**, e1501286 (2016).
- [20] Y. Tabuchi, S. Ishino, A. Noguchi, T. Ishikawa, R. Yamazaki, K. Usami, and Y. Nakamura, *Science* **349**, 405 (2015).
- [21] D. Lachance-Quirion, S. P. Wolski, Y. Tabuchi, S. Kono, K. Usami, and Y. Nakamura, *Science* **367**, 425 (2020).
- [22] Y. Tabuchi, S. Ishino, A. Noguchi, T. Ishikawa, R. Yamazaki, K. Usami, and Y. Nakamura, *C. R. Phys.* **17**, 729 (2016).
- [23] Y. M. Bunkov, *J. Exp. Theor. Phys.* **131**, 18 (2020).
- [24] A. Kamra, W. Belzig, and A. Brataas, *Appl. Phys. Lett.* **117**, 090501 (2020).
- [25] P. Pirro, V. I. Vasyuchka, A. A. Serga, and B. Hillebrands, *Nat. Rev. Mater.* **6**, 1114 (2021).
- [26] H. Y. Yuan, Y. Cao, A. Kamra, R. A. Duine, and P. Yan, *Phys. Rep.* **965**, 1 (2022).
- [27] T. Kampfrath, A. Sell, G. Klatt, A. Pashkin, S. Mährlein, T. Dekorsy, M. Wolf, M. Fiebig, A. Leitenstorfer, and R. Huber, *Nat. Photonics* **5**, 31 (2011).
- [28] T. Jungwirth, X. Marti, P. Wadley, and J. Wunderlich, *Nat. Nanotechnol.* **11**, 231 (2016).
- [29] F. Keffer and C. Kittel, *Phys. Rev.* **85**, 329 (1952).
- [30] A. Einstein, B. Podolsky, and N. Rosen, *Phys. Rev.* **47**, 777 (1935).
- [31] S. K. Kim, G. S. D. Beach, K.-J. Lee, T. Ono, Th. Rasing, and H. Yang, *Nat. Mater.* **21**, 24 (2022).
- [32] K.-J. Kim, S. K. Kim, Y. Hirata, S.-H. Oh, T. Tono, D.-H. Kim, T. Okuno, W. S. Ham, S. Kim, G. Go, Y. Tserkovnyak, A. Tsukamoto, T. Moriyama, K.-J. Lee, and T. Ono, *Nat. Mater.* **16**, 1187 (2017).
- [33] S.-H. Oh, S. K. Kim, D.-K. Lee, G. Go, K.-J. Kim, T. Ono, Y. Tserkovnyak, and K.-J. Lee, *Phys. Rev. B* **96**, 100407(R) (2017).
- [34] J. Shim, S.-J. Kim, S. K. Kim, and K.-J. Lee, *Phys. Rev. Lett.* **125**, 027205 (2020).
- [35] Ö. O. Soykal and M. E. Flatté, *Phys. Rev. Lett.* **104**, 077202 (2010).
- [36] H. Huebl, C. W. Zollitsch, J. Lotze, F. Hocke, M. Greifenstein, A. Marx, R. Gross, and S. T. B. Goennenwein, *Phys. Rev. Lett.* **111**, 127003 (2013).
- [37] X. Zhang, C.-L. Zou, L. Jiang, and H. X. Tang, *Phys. Rev. Lett.* **113**, 156401 (2014).
- [38] Y. Tabuchi, S. Ishino, T. Ishikawa, R. Yamazaki, K. Usami, and Y. Nakamura, *Phys. Rev. Lett.* **113**, 083603 (2014).
- [39] L. Bai, M. Harder, Y. P. Chen, X. Fan, J. Q. Xiao, and C.-M. Hu, *Phys. Rev. Lett.* **114**, 227201 (2015).
- [40] V. L. Grigoryan, K. Shen, and K. Xia, *Phys. Rev. B* **98**, 024406 (2018).
- [41] B. Bhoi, B. Kim, S.-H. Jang, J. Kim, J. Yang, Y.-J. Cho, and S.-K. Kim, *Phys. Rev. B* **99**, 134426 (2019).
- [42] Y. Li, T. Polakovic, Y.-L. Wang, J. Xu, S. Lendinez, Z. Zhang, J. Ding, T. Khaire, H. Saglam, R. Divan, J. Pearson, W.-K. Kwok, Z. Xiao, V. Novosad, A. Hoffmann, and W. Zhang, *Phys. Rev. Lett.* **123**, 107701 (2019).
- [43] J. T. Hou and L. Liu, *Phys. Rev. Lett.* **123**, 107702 (2019).
- [44] W. Yu, J. Wang, H. Y. Yuan, and J. Xiao, *Phys. Rev. Lett.* **123**, 227201 (2019).
- [45] H. Y. Yuan and X. R. Wang, *Appl. Phys. Lett.* **110**, 082403 (2017).
- [46] M. Mergenthaler, J. Liu, J. J. Le Roy, N. Ares, A. L. Thompson, L. Bogani, F. Luis, S. J. Blundell, T. Lancaster, A. Ardavan, G. A. D. Briggs, P. J. Leek, and E. A. Laird, *Phys. Rev. Lett.* **119**, 147701 (2017).
- [47] Ø. Johansen and A. Brataas, *Phys. Rev. Lett.* **121**, 087204 (2018).
- [48] R. Schnabel, *Phys. Rep.* **684**, 1 (2017).
- [49] S. Flügge, *Encyclopedia of Physics*, vol. 18/2 (Springer-Verlag, Berlin, 1966).
- [50] T. Holstein and H. Primakoff, *Phys. Rev.* **58**, 1098 (1940).
- [51] N. N. Bogoljubov, *Nuovo Cim.* **7**, 794 (1958).
- [52] R. F. Bishop and A. Vourdas, *Z. Phys. B* **71**, 527 (1988).
- [53] L. Néel, *Ann. Phys. (Paris)* **5**, 232 (1936).
- [54] See Supplemental Material at <http://link.aps.org/supplemental/10.1103/PhysRevB.106.L140408> for spin-flop field, $E_N^{(s)}$ without photon, Hamiltonian of photon coupled magnon system, $E_N^{(s)}$ between magnon modes of the photon coupled system, magnon entanglement of FIMs, FMs and AFMs, effect of the bath temperature, effect of dissipation rates of modes, and candidates for ferrimagnet to realize the enhanced magnon-magnon entanglement.
- [55] C. Kim, S. Lee, H.-G. Kim, J.-H. Park, K.-W. Moon, J. Y. Park, J. M. Yuk, K.-J. Lee, B.-G. Park, S. K. Kim, K.-J. Kim, and C. Hwang, *Nat. Mater.* **19**, 980 (2020).
- [56] M. Deb, P. Molho, and B. Barbara, *Phys. Rev. B* **105**, 014432 (2022).
- [57] P. Chaudhari, J. J. Cuomo, and R. J. Gambino, *Appl. Phys. Lett.* **22**, 337 (1973).
- [58] A. Hrabec, N. T. Nam, S. Pizzini, and L. Ranno, *Appl. Phys. Lett.* **99**, 052507 (2011).

- [59] C. Du, T. van der Sar, T. X. Zhou, P. Upadhyaya, F. Casola, H. Zhang, M. C. Onbasli, C. A. Ross, R. L. Walsworth, Y. Tserkovnyak, and A. Yacoby, *Science* **357**, 195 (2017).
- [60] K. Agarwal, R. Schmidt, B. Halperin, V. Oganesyan, G. Zaránd, M. D. Lukin, and E. Demler, *Phys. Rev. B* **95**, 155107 (2017).
- [61] B. Flebus and Y. Tserkovnyak, *Phys. Rev. Lett.* **121**, 187204 (2018).
- [62] T. Okuno, D.-H. Kim, S.-H. Oh, S. K. Kim, Y. Hirata, T. Nishimura, W. S. Ham, Y. Futakawa, H. Yoshikawa, A. Tsukamoto, Y. Tserkovnyak, Y. Shiota, T. Moriyama, K.-J. Kim, K.-J. Lee, and T. Ono, *Nat. Electron.* **2**, 389 (2019).
- [63] D. F. Walls and G. J. Milburn, *Quantum Optics*, 2nd ed. (Springer, Berlin, 2008).
- [64] E. X. DeJesus and C. Kaufman, *Phys. Rev. A* **35**, 5288 (1987).
- [65] M. Imai, Y. Ogata, H. Chudo, M. Ono, K. Harii, M. Matsuo, Y. Ohnuma, S. Maekawa, and E. Saitoh, *Appl. Phys. Lett.* **113**, 052402 (2018).
- [66] L. Caretta, S.-H. Oh, T. Fakhru, D.-K. Lee, B. H. Lee, S. K. Kim, C. A. Ross, K.-J. Lee, and G. S. D. Beach, *Science* **370**, 1438 (2020).
- [67] J. Zhao, A. V. Bragas, D. J. Lockwood, and R. Merlin, *Phys. Rev. Lett.* **93**, 107203 (2004).
- [68] A. A. Clerk, K. W. Lehnert, P. Bertet, J. R. Petta, and Y. Nakamura, *Nat. Phys.* **16**, 257 (2020).